Int. J. Electrochem. Sci., 16 **(2021)** Article ID: 210359, doi: 10.20964/2021.03.05

International Journal of
ELECTROCHEMICAL
SCIENCE
www.electrochemsci.org

Biomass Carbon Materials Derived from Starch and their Electrochemical Properties

Yawen Hu, Xin Li, Guoying Wang, Fenfang Luo, Kaiqiang Yi, Yves Iradukunda, Gaofeng Shi[*]

School of Petrochemical Engineering, Lanzhou University of Technology, Lan gong ping Road, Lanzhou, Gansu, China
[*]E-mail: 1063623387@qq.com

Received: 30 September 2020 / *Accepted:* 17 November 2020 / *Published:* 31 January 2021

Porous carbon was prepared by using starch as a carbon source and $ZnCl_2$ as an activator. The physical and chemical properties of porous carbon materials were characterized by scanning electron microscope (SEM), transmission electron microscope (TEM), X-ray diffraction (XRD), Raman spectroscopy, Nitrogen adsorption/desorption, and XPS. Nitrogen adsorption/desorption tests show that $ZnCl_2$ has well pore expansion, with a maximum specific surface area of 1591.83 m^2 /g and a total pore volume of 0.89 cm^3/g. Under the 1A/g current density, the specific capacitance is 249F/g. When the current density gains from 1A/g to 10 A/g, the capacitance retention reaches 72.29%. At the same time, it demonstrates high energy density (34.34 W·h/g) and power density (500W·K/g). The capacitance retention is 90.4% after 5000 cycles at 2 A/g current density. The results depict that the porous carbon is not only an ideal electrode material for supercapacitors but also a good carrier for the preparation of catalysts from mesoporous materials.

Keywords: starch, porous carbon, electrochemical performance, supercapacitor

1. INTRODUCTION

With the rapid development of the social economy and the speedy improvement of human living standards, the consumption of energy is rising. Force the world to develop green and sustainable new energy and explore containers that effectively store these renewable energies to generate electricity. In various energy storage devices, batteries and supercapacitors represent two leading electrochemical energy storage technologies [1]. Supercapacitors, also known as electrochemical capacitors, compared with batteries, supercapacitors can safely provide high power and fast charge/discharge [2,3] and have an extremely long cycle life and flexible operation. It has attracted more and more attention and research of researchers all over the world. The growth of electrode materials with excellent electrochemical

performance for supercapacitors is the top priority to improve the electrochemical performance of supercapacitors. Compared with other supercapacitor electrode materials, carbon materials receive a relatively low price and are most likely to accomplish industrial production. Moreover, carbon materials have the advantages of stable chemical properties, Rich pore structure, large specific surface area, and without pollution [4].

Since Becker applied to use activated carbon as electrode material for electric double-layer capacitors in 1957, the main carbon electrode materials for supercapacitors are activated carbon [5], activated carbon fiber [6], carbon nanotubes [7], carbon nanospheres [8], graphene [9], template carbon [10] and so on.

Biomass carbon materials come from a wide range of sources, utilizing all kinds of carbon-rich substances in nature, such as plants, animal manure, animal bones, agricultural and forestry wastes, as precursors, prepared by high-temperature carbonization and activation. There are lots of pore structures in the biomass material itself, and the pores are further expanded and extended through physical and chemical activation to obtain carbon materials with rich pores [11]. These natural advantages make it advantageous to be used in supercapacitor electrode materials and get the attention of relevant researchers. Due to the characteristics of biomass raw materials, different biomass precursors require different methods to prepare carbon materials with the best electrochemical performance.

The carbon sources commonly used as porous carbon are plant residues, domestic wastes, and so on. Gao. [12] prepared porous carbon with rice husk as a precursor and KOH as an activator. In tetraethylammonium tetrafluoroborate electrolyte, the specific capacitance of porous carbon can reach 174F/g [13]. Using waste plastic bottles as a precursor, carbon material was prepared by the direct-carbonization method. The specific capacitance can reach 176 F/ g at 1 A/g current density. Chen. [14] prepared electrode materials for supercapacitors with tobacco waste as the premise and KOH as the activator. The specific capacitance can reach 148 F/g at 0.5 A/g current density.

As a renewable carbon source with high carbon content, starch exists in large amounts in nature and is easy to obtain. Using starch as a carbon source is beneficial to industrial production. Jin. [15] obtained Spherical type carbon with the high specific surface area through stabilization, carbonization, and KOH activation using cassava starch as a precursor. Qiang. [16] prepared highly dispersed carbon microspheres by hydrothermal carbonization and high-temperature heat treatment applying potato starch as the precursor. As the electrode material of supercapacitors, the specific capacitance of the microspheres can reach 245F/g at 1A/g current density. Peng. [17] employed corn starch as a precursor and H_3PO_4 as an activator to prepare porous carbon materials. The specific capacitance can reach 162F/g at 0.652 A/g current density.

Researchers have been working hard to enhance the specific surface area of carbon electrode materials for supercapacitors and establish a reasonable pore structure distribution. The activation methods of carbon electrode materials are mainly divided into physical activation method and chemical activation method. Physical activation is the use of water vapor, carbon dioxide, supercritical water, and other oxidizing gases to open the originally blocked pores in carbon materials, and further expand and make pores to form a new pore structure [18-20]. This method has the advantages of a simple pore expansion process of activated carbon and little environmental pollution, and the products can be applied directly without repeated cleaning. This method is mainly used to produce activated carbon in the

industry[21]. Chemical activation expends KOH, NaOH, $ZnCl_2$, H_3PO_4, and transition metal salts (such as iron salt, nickel salt, cobalt salt, nitrate, borate, etc.) as activators. Activated carbon materials with developed pores and high specific surface area can be obtained by adding activators according to a certain proportion in the process of precursor carbonization[22].

In this research, starch was applied as a carbon source and $ZnCl_2$ as an activator to prepare porous carbon. Simultaneously, the effect of the amount of $ZnCl_2$ activator on the properties of porous carbon was controlled. The prepared materials were used as supercapacitor electrode materials to analyze their electrochemical properties. Under the 1A/g current density, the specific capacitance can reach 249 F/g, and the capacitance retention rate of the 5000 charge/discharge cycle is 90.4% at 2 A/g current density, demonstrating well cycle stability.

2. EXPERIMENTAL

2.1. Experimental method

The starch utilized in this experiment is soluble starch (Wuxi Yatai United Chemical Co., Ltd.). Zinc chloride (Tianjin Damao Chemical Reagent Factory) is analytically pure. Porous carbon was prepared by activation of zinc chloride and mixed with $ZnCl_2$ and starch. the mass ratio of starch to $ZnCl_2$ was 1:0, 1:1, 1:2 and 3:2. Then the solid mixture was heated to 800 ℃ under the protection of nitrogen in a high-temperature tube furnace and the activation time was 2h. Finally, the black solid product was washed to neutral with 1M/L HCl and dried in a vacuum oven to obtain graded porous carbon. The porous carbon was named as follows: SC-X, SC-1 is the mass ratio of starch to $ZnCl_2$ is 1:0, SC-2 is the mass ratio of starch to $ZnCl_2$ is 1:1, SC-3 is the mass ratio of starch to $ZnCl_2$ is 2:1, and SC-4 is the mass ratio of starch to $ZnCl_2$ is 3:2.

2.2. Structural characterization

The micromorphology of the samples was observed by scanning electron microscope (SEM; MIRA3; TESCAN). The pore size distribution and specific surface area of the samples were measured by nitrogen adsorption measurement Brunauer - Em - mett - Teller (BET) in Micromeritics ASAP 2420 surface analyzer. The crystal structure of the material was tested by MSAL-XD2 powder X-ray diffractometer (the scanning range of diffraction angle is 580°). The functional groups of the samples were detected by Lab RAM HR Evolution confocal Raman spectrometer.

2.3. Electrochemical test

The electrochemical performance was measured by three electrodes of CHI 660D electrochemical workstations, and the electrolyte was KOH solution with a concentration of 6mol/L. The obtained sample was uniformly mixed with acetylene black and polytetrafluoroethylene (PTFE) according to the mass ratio of 80%, 15%, 5% to prepare the working electrode. The full mixed sample

is uniformly coated on a 2×1 cm nickel sheet with a coverage area of 1×1cm. The prepared working electrode was dried at 80℃ for 8 h in a vacuum drying box, and then the electrode was made under the pressure of 6m Pa. Utilizing saturated calomel electrode (SCE) as a reference electrode and platinum foil as the counter electrode, cyclic voltammetry (CV), constant current charge-discharge (GCD) and impedance (EIS) was carried out on electrochemical workstation. Constant current charge/discharge (GCD) measurements were performed at densities ranging from 0.5 A/g to 10 A/g, and cyclic voltammetry (CV) measurements were carried out at scan rates from 5 mV /s to 100 mV/s. The voltage range measured by CV and GCD is-1V- 0V. The specific capacitance C (F/g), energy density E (Wh Kg^{-1}), and power density P (W Kg^{-1}) are calculated using the following formula:

$$C = \frac{i\Delta t}{m\Delta V} \quad (1)$$

$$E = \frac{1}{2} C \Delta V^2 \quad (2)$$

$$P = \frac{E}{\Delta t} \quad (3)$$

Where i (A) is the discharge current, Δt (s) is the discharge time, m (g) is the mass of the active material of a single electrode, and ΔV (V) is the voltage range [21,22]

3. RESULTS AND DISCUSSION

3.1. Surface morphologies

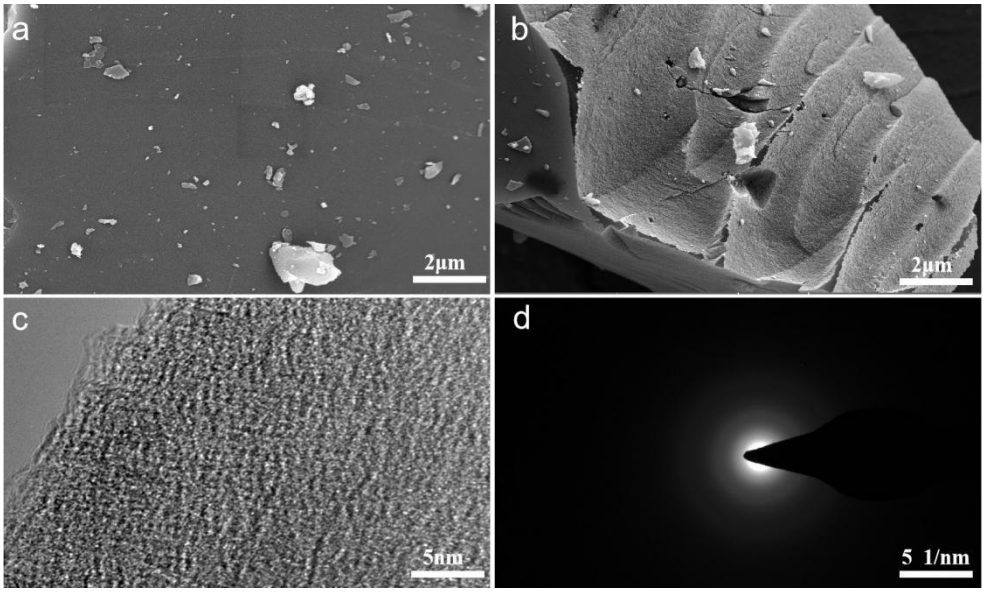

Figure 1. SEM micrographs of (a) SC-1 (b) SC-4and(c)SC-4 ; TEM

The microstructure of the prepared carbon materials was observed by SEM and TEM. By magnifying the SEM image at 2500 times, it can be discovered that the surface structure of the carbon material without $ZnCl_2$ activation is smooth and there is no obvious void (Fig.1a). Under the same magnification, the carbon material activated by $ZnCl_2$ appears massive structure, a rough outer surface, and irregular shape (Fig.1b). By further magnifying the TEM image at 1000000 times, it can be seen

that the surface of the carbon material activated by $ZnCl_2$ is rich in micropore structure (Fig.1c). The formation of this surface is beneficial to the ion storage and migration of the electrolyte, and a double electric layer is formed on the surface of the carbon electrode. As a result, it depicts a higher specific capacity and better electrochemical performance.

3.2. XRD and Raman analysis

The crystal structure and graphitization degree of all samples were characterized by XRD and Raman spectra. Figure.2a is the crystal structure diagram of XRD with different amounts of $ZnCl_2$. Through XRD characterization, two wide diffraction peaks were observed at 22 °and 43 °, corresponding to the (002) and (100) crystal planes of graphite carbon, respectively. There is a wide peak at 2θ, which indicates that the regularity of the crystal structure increases, indicating that the prepared material belongs to the amorphous graphite structure[23]. Besides, with the increase of $ZnCl_2$ mass, the diffraction peak intensity of carbon materials continues to strengthen, indicating that the degree of graphitization increases, and the degree of amorphous decreases[24].

The Raman test can be used to analyze the degree of graphitization of carbon. Figure.2b displays the Raman test results of all samples. It can be viewed from the diagram that there are two obvious characteristics peaks the D peak and the G peak, in which the D peak represents the disordered structure of carbon materials, and the G peak represents the graphitized structure [25]. The intensity ratio of D band to G band can reflect the degree of structural disorder in carbon materials, and the graphitization degree of carbon matrix is analyzed [26]. The ID/ IG values of SC-1, SC-2, SC-3 and SC-4 were 0.94,0.89,0.88,0.83 respectively. The results show that the degree of graphitization increases with the increase of the quality of $ZnCl_2$, which is consistent with the results of XRD analysis. Affected by this crystal form, the ion in the electrolyte is transported rapidly, which enhances the conductive ability of carbon materials, thus improving the electrochemical performance of carbon materials.

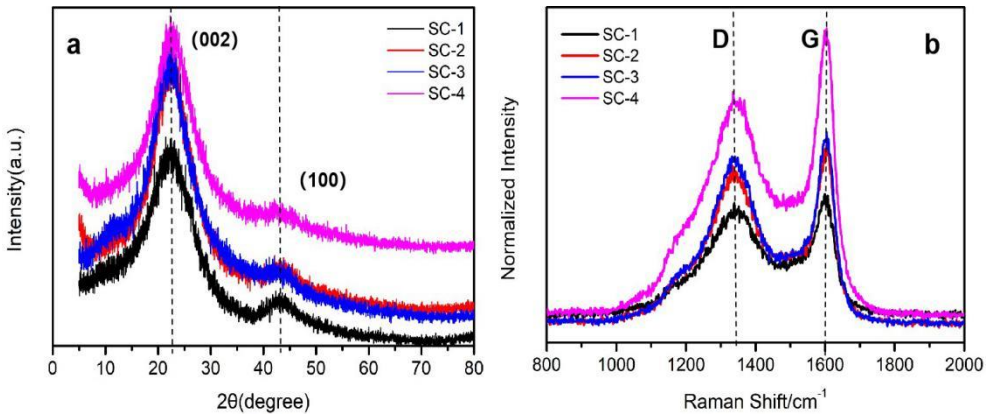

Figure 2. (a) XRD patterns of the samples, (b) Raman spectra of the samples

3.3. Analysis of specific surface area and pore structure

To further analyze the distribution of the interstitial structure of the materials, the samples were characterized by nitrogen adsorption-desorption, and the results are as shown in Figure.3a. According to IUPAC classification, porous carbon shows a type IV adsorption/desorption isotherm. The sharp increase of the adsorption volume of SC-4 at lower relative pressure indicates that there are a large number of micropores. At higher relative pressure, the existence of mesopores leads to a retention ring in the nitrogen adsorption-desorption curve and an upward trend at the end of the curve, indicating that there is still a large pore structure. The analysis results are consistent with SEM images and TEM images. Figure.3b is the (PSD) curve of pore size distribution calculated by the Barrett-Joyner-Halenda (BJH) method. Porous carbon shows a rich microporous structure.

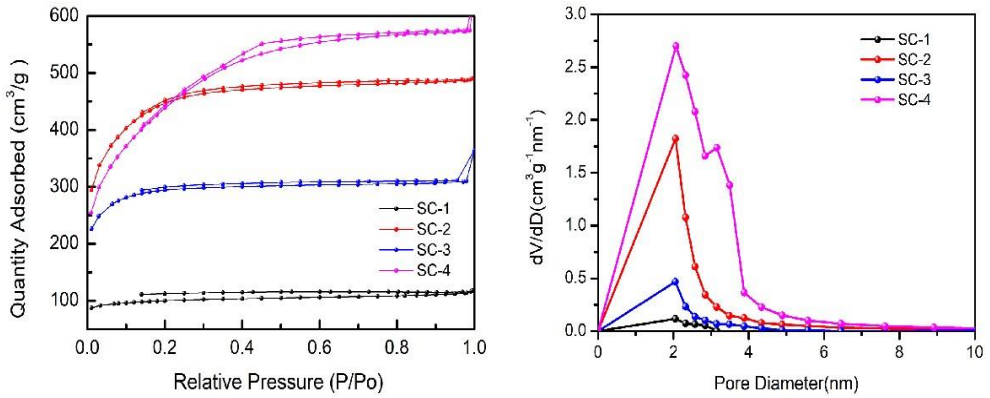

Figure 3. (a) N_2 adsorption/desorption isotherms and (b) the BJH pore size distribution curves of the porous carbons.

The void structures of different proportions of $ZnCl_2$ porous carbon are listed (Table1). It can be seen from the surface that the specific surface area of the sample SC-4 is 1591.83 m^2/g and the total pore volume is 0.89 cm^3/g. The micropore specific surface area of 550.52 m^2/g accounts for 35.6% of the total specific surface area, and the micropore volume of 0.38 cm^3/g accounts for 42.7% of the total pore volume. The results prove that there are more micropores in the structure of porous carbon.

Table 1. The pore size distribution of porous carbon

Sample	S_{BET}[a] ($cm^2 \cdot g^{-1}$)	V_c[b] ($cm^3 \cdot g^{-1}$)	D_{ave}[c] (nm)	V_{mic}[d] ($cm^3 \cdot g^{-1}$)	V_{ext}[e] ($cm^3 \cdot g^{-1}$)	S_{mic}[f] ($cm^2 \cdot g^{-1}$)	S_{ext}[g] ($cm^2 \cdot g^{-1}$)
SC-1	337.34	0.175	2.08	0.12	0.06	256.52	80.82
SC-2	1577.92	0.75	1.91	0.28	0.47	648.43	929.49
SC-3	1004.62	0.48	1.90	0.33	0.15	730.05	274.57
SC-4	1591.83	0.89	2.23	0.38	0.51	550.52	1041.31

a: BET surface area; b: Total pore volume; c: Average pore diameter; d: Micropore volume; e: External volume; f: Micropore surface area; g: External surface area

3.5. XPS characterization

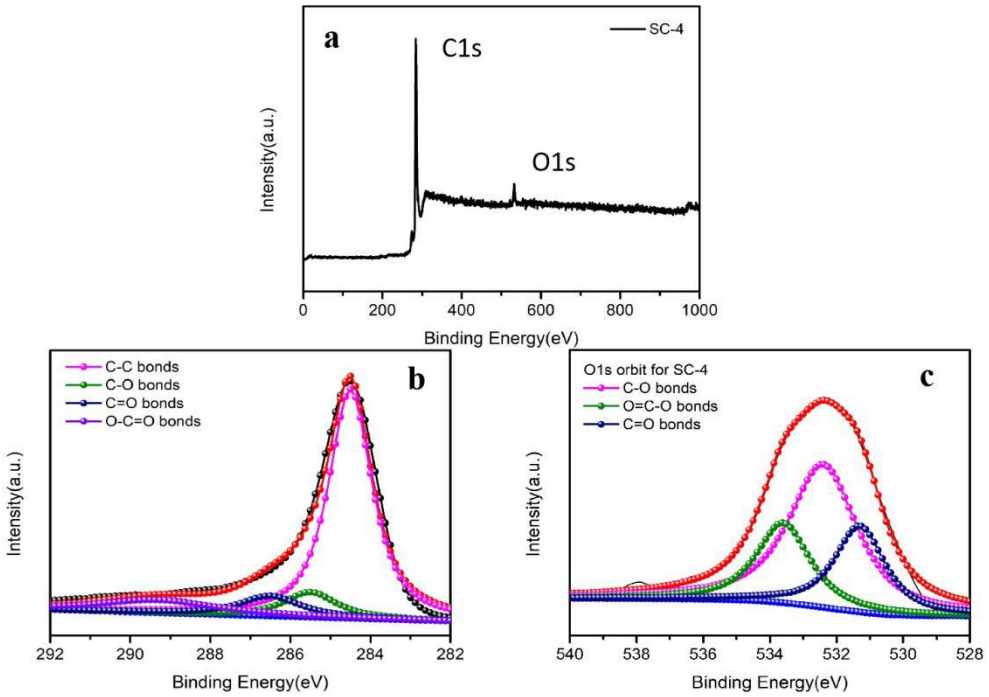

Figure 4. XPS full peak, C1s and O1s spectra of the SC-4 sample

To determine the elemental composition and bonding of the sample, the sample SC-4 was analyzed by X-ray photoelectron spectroscopy (XPS). The content of C, O, and N in the SC-4 sample is C 95.51 wt%, O 3.62 wt%, N 0.82 wt%, which indicates that porous carbon almost does not contain N element. Figure.4a shows the full peak of the SC-4 sample, from which we can discover that there are only C peak and O peak.

For the C1s XPS spectrum (Figure.4b), SC-4 samples can be synthesized into three parts. Carbon is mainly bonded to neighboring C or H by Sp^2 hybridization (284.6 eV), and O connected C-O bond (285.5 eV), and C=O (286.5 eV) and COOH bond (289.3 eV) [27]. For the O1s XPS pattern (Figure.4c), SC-4 samples can be synthesized into three parts. They are the double-bonded oxygen in the C=O group at 531.6 eV, the singly bonded oxygen (-O-) in the C-O group at 532.7 eV, and the oxygen in the carboxyl group at 533.7 eV (O=C-O) [28]. Generally speaking, the bonding form is mainly combined with O=C-O. Part of the C element of the sample exists in the form of oxygen-containing functional groups. The existence of oxygen-containing functional groups on the surface of the electrode material can improve the electrochemical performance of the electrode material because it gains the hydrophilicity of the electrode material. Can contact with the electrolyte more completely.

3.6. Electrochemical analysis

Figure.5a is a constant current charge-discharge electrogram with different activating agent ratio at 0.5A/g current density. As can be seen from the figure, all the samples are in the shape of an isosceles triangle. And it can be seen from the figure that there is no voltage drop, which shows that the prepared

electrode material has good reversibility in the process of electrochemical testing. Under the current density of 1A/g, the specific capacitances of SC-1, SC-2, SC-3, and SC-4 are 70F/g, 178.6F/g, 171.3F/g, and 245.3 FMCG, respectively. The results express that the discharge time of the GCD curve increases at first and then decreases with the increase of $ZnCl_2$, which is consistent with the result of the CV curve. Table 2 demonstrates the specific capacitance of SC-1, SC-2, SC-3, SC-4 at different current densities.

Table 2. Specific capacitance values of each sample at different current densities (F/g)

Current density (A/g)	0.5	1	2	3	4	5	6	7	8	9	10
SC-1	90.1	70.0	55.7	50.2	45.1	40.1	38.3	35.6	32.9	30.1	28.0
SC-2	197.6	178.6	167.0	160.3	157.7	153.7	149.8	144.0	140.2	137.8	135.2
SC-3	218.1	171.3	154.3	149.9	144.3	141.9	139.2	137.6	135.9	133.8	132.0
SC-4	272.5	245.3	225.5	217.3	205.6	196.5	192.0	188.4	184.1	179.9	177.7

To trial, the electrochemical performance of the prepared sample, porous carbon was prepared as the electrode material, and the three-electrode system was assembled with 6M/L KOH solution as the electrolyte to test the electrochemical performance of supercapacitors (Figure.5). Figure.5b is a cyclic voltammetry curve (CV) with different activator ratios at a scanning rate of 20 mV/s. It can be discovered from the figure that the cyclic voltammetry curve of SC-1 of the sample without $ZnCl_2$ activation is different from that of the sample with $ZnCl_2$. The cyclic voltammetry curve of all the samples with $ZnCl_2$ presents a quasi-rectangular shape, and without redox peak, indicating that the material has typical double-layer capacitance characteristics [29]. However, the curve of the sample without $ZnCl_2$ is triangular, indicating that it has no double-layer capacitance, indicating that the sample activated by $ZnCl_2$ has an ideal double-layer capacitance and large charge storage capacity. The results depicted that with the increase of the mass ratio of starch to $ZnCl_2$, the closed area of the CV curve increased at first and then decreased, indicating that the curve area of the SC-4 sample was the largest and the electrochemical performance was the best.

From Figure.5d and Table.2, when the current density increases from 1 A/g to 10 A/g, the specific capacitances of SC-1, SC-2, SC-3, and SC-4 samples decrease to 31.1%, 68.4%, 60.5%, and 70.8% of the initial values, respectively. Thus, it can be seen that the activation of $ZnCl_2$ can promote the rate performance of the samples.

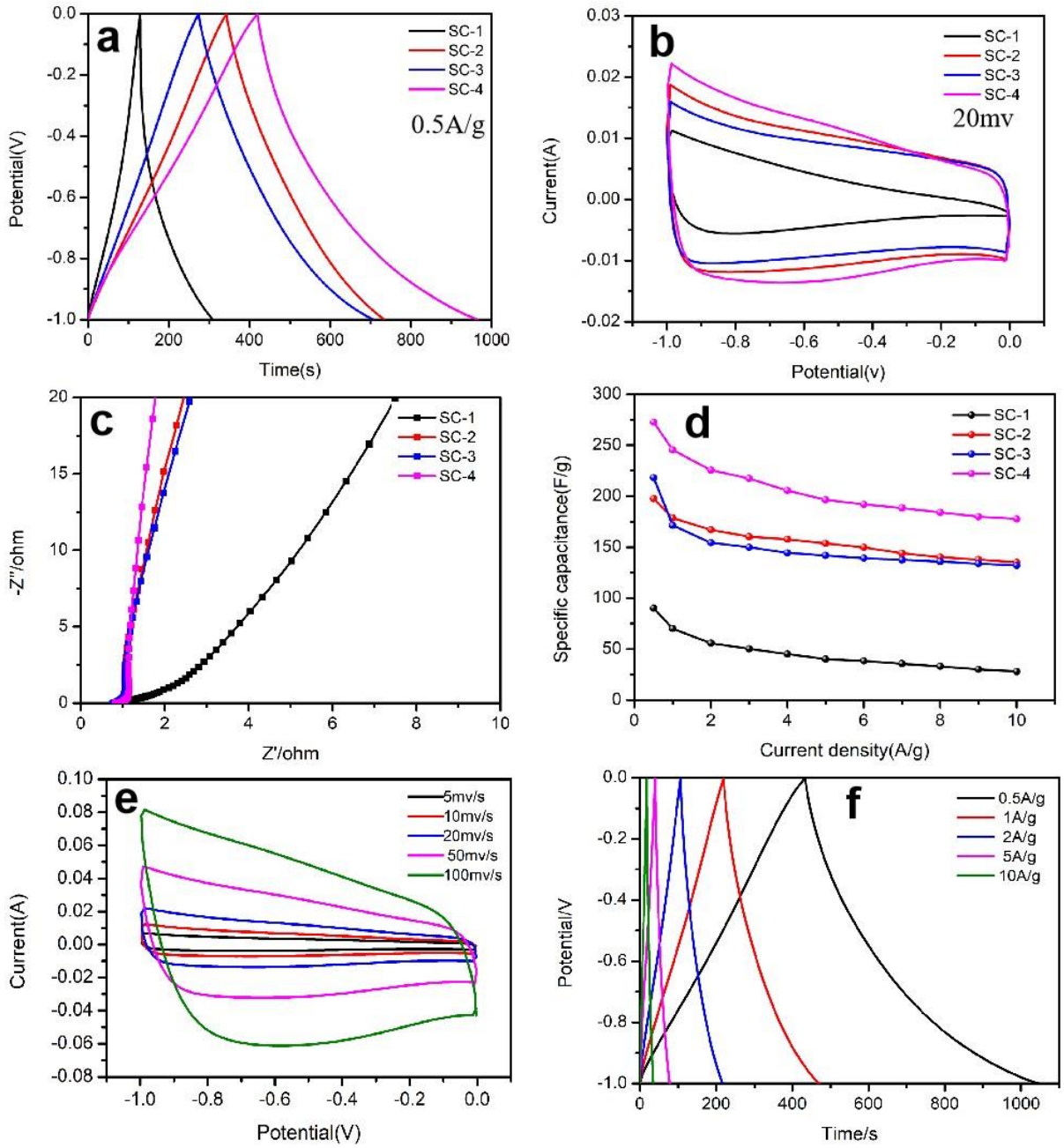

Figure 5. Electrochemical performance of the samples measured in a three-electrode system: (a) GCD curves of all the samples at the current density of 0.5A/g ;(b) CV curves for all the samples at a scan rate of 20 mV/s (c) Electrochemical impedance spectra (EIS);(d) specific capacitance of the samples versus various current densities from 0.5 to 10 A/g;(e) CV curves for SC-4 at scan rates ranging from 5 to 100 mV/s ; (f) GCD curves of SC-4 at different current densities.

To further understand the electrochemical properties of three kinds of activated carbon materials, EIS measurements were carried out, and the results are shown in Figure.5c. In the high-frequency region, the point crossing with the real axis reflects that the internal resistance (Rs), the semicircle of the electrode material corresponds to the charge transfer resistance. The approximate vertical line in the low-frequency region represents the diffusion resistance (W) of the electrolyte in the porous structure [30]. It expresses that the electrolyte solution has well transport and diffusion properties in the prepared

materials, and the sample SC-4 is closer to the vertical axis in the low-frequency region, indicating that SC-4 has the best transport and diffusion properties among all samples.

Figure.5e is the CV curve of sample SC-4 at different scanning rates. It can be considered from the figure that the cyclic voltammograms at all scanning speed are quasi-rectangular, and the quasi-rectangle remains unchanged even when the scanning speed increases to 100 mV/s. The results demonstrate that the prepared porous carbon electrode materials have good ion transport capacity in the electrolyte and maintain good rate performance at high scanning speed. Figure.5f is the specific capacitance of SC-4 at different current densities. the figure presents the charge-discharge curves of the prepared porous carbon are isosceles-like triangles at different current densities. With the growth of the current density, the time of charge and discharge becomes shorter, because the ion in the electrolyte shuttles through the pores of the electrode material will be limited under the high current density so that the specific capacitance decreases.

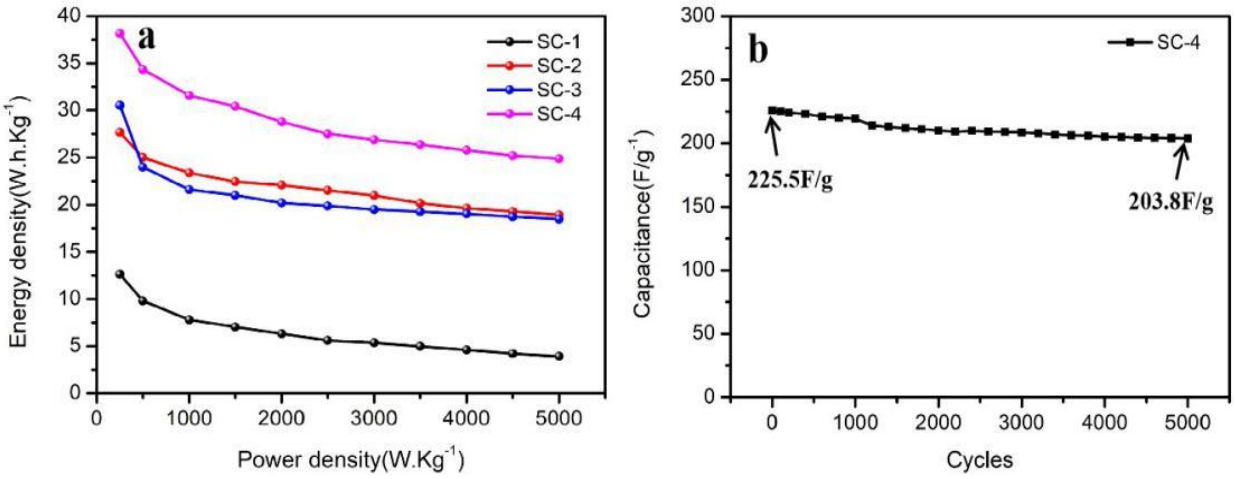

Figure 6. (a) Energy and power density of the samples; (b) SC-4 in specific capacitance retention rates at 2 A/g after 5000 cycle

Figure.6a shows that porous carbon SC-4 receive the highest current density and power density at the same current density, and the energy density is 24.88W·h K/g when the energy density is 34.34W·h K/g, power density 5000W·K/g at 500W·K/g. This is because the SC-4 sample has good electrical conductivity, promotes electron transfer, and is beneficial to the increase of energy density.

The cycle characteristic diagram of the SC-4 sample is shown from Figure.6b at a current density of 2A/g, after 5000 charge-discharge cycles, the specific capacitance of the SC-4 sample is 203.8 F/g, and the retention rate is 90.4%, indicating that the sample has good electrochemical cycle stability.

To evaluate the superiority of the prepared electrode materials, Table 3 lists our results compared to previously published preparations of porous carbon by starch.

Table 3. Comparison of electrochemical performance of porous carbon with other different materials

Electrode materials	Specific capacitance (current density)	Electrolyte	Referencces
porous carbon based on cationic starch	238 $F \cdot g^{-1}$ (0.37 $A \cdot g^{-1}$)	30wt% KOH	[31]
porous carbon based on potato starch	245 $F \cdot g^{-1}$ (1 $A \cdot g^{-1}$)	1 $mol \cdot L^{-1}$ KOH	[17]
porous carbon based on corn starch	162 $F \cdot g^{-1}$ (0.652 $A \cdot g^{-1}$)	6 $mol \cdot L^{-1}$ KOH	[32]
porous carbon based on corn starch	249 $F \cdot g^{-1}$ (1 $A \cdot g^{-1}$)	6 $mol \cdot L^{-1}$ KOH	This work

4. CONCLUSION

Porous carbon materials were prepared with corn starch as carbon source and $ZnCl_2$ as an activator, and the morphology, microstructure, and electrochemical properties of porous carbon under different activation conditions were investigated. By controlling the amount of $ZnCl_2$, the sample SC-4 with the best electrochemical performance was obtained. The specific capacitance of porous carbon is 255.5 F/g when the current density is 1 A/g, and the energy density is 34.34 W·h/g when the power density is 500 W/g. The capacitance retention rate is 70.8%, which has a good rate of performance. After 5000 cycles of charge and discharge, the capacitance value is maintained at 90.4%, with excellent cycle stability. SC-4 has a high specific surface area and exists in the form of a large number of micropores and mesopores. SC-4 porous carbon is not only a good electrode material for supercapacitors but also a good carrier for mesoporous materials to prepare catalysts.

References

1. B. G. Choi, J. Hong, W. H. Hong,P. T. Hammond and H. S. Park, *ACS Nano*, 5(2011)7205.
2. A. G. Snook, P. Kao and A. S. Best, *J. Power Sources*, 196(2011)1.
3. F. Meng, J. Li, S. K. Cushing, M. Zhi and N. Wu, *Nanoscale*, 5(2013)1.
4. Z. Wang, Y. Tan, Y. Yang, X. Zhao, Y. Liu, L. Niu,T. Brandon, L. Kong, L. Kang, Z. Liu and F. Ran, *J. Power Sources*, 378(2018)499.
5. E. Frackowiak and F. Béguin, *Carbon*, 40(2002)1775.
6. M. H. Al-Saleh and U. Sundararaj, *Carbon*, 47(2009)2.
7. H. Shan, R. Rajamani and Y. Xun, *Appl. Phys. Lett.*, 100(2012)103.
8. X. Zhang, Z. Sui, B. Xu, Y. Luo, W. Zhan and B. Liu, *J. Mater. Chem.*, 21(2011)6494.
9. R. Rinaldo, V. Alberto, P. Stefano, S. Bruno, *Nat. Mater.*, 14(2015)271.
10. C. O. Ania, V. Khomenko, E. Raymundo-Pinero, J. B. Parra and F. Béguin, *Adv. Funct. Mater.*, 17(2010)1828.
11. X. Wang, X. Chen and Y. Zhang, *Stat. Probabil. Lett.*, 102(2018)135.
12. Y. Gao, L. Li, Y. Jin, Y. Wang, C. Yuan, Y. Wei, G. Chen, J. Ge and H. Lu, *Appl. Energ.*,153(2015)41.
13. X. Zhao, P. Li, S. Yang, Q. Zhang and H. Luo, *Ionics*, 23(2017)1239.

14. S. Zhao, C. Wang, M. Chen and Z. Shi, *Mater. Lett.*, 62(2008)3322.
15. S. Zhao, C. Wang, M. Chen, Z. Shi and N. Liu, *New Carbon Mater.*, 25(2010)438.
16. D. Jin, X. Yang, M. Zhang, B. Hong, H. Jin, X. Peng, J. Li, H. Ge, X. Wang, Z. Wang and H. Lou, *Mater. Lett.*, 139(2015)262.
17. R.B. Qiang, Z.A. Hu, Y.Y. Yang, Z.M. Li, A. Ning, X.Y. Ren, H.X. Hu and H.Y. Wu, *Electrochim. Acta*, 167 (2015) 303.
18. C. Bouchelta, M. S. Medjram, O. Bertrand and J. Bellat, *J. Anal. Appl. Pyrolysis*, 82(2008)70.
19. M. S. Shafeeyan, W. M. A. W. Daud, A. Houshmand and A. Shamiri, *J. Anal. Appl. Pyrolysis*, 89(2010)143.
20. M. Molina-Sabio, M.T. Gonzalez, F. Rodriguez-Reinoso and A. Sepúlveda-Escribano, *Carbon*, 34(1996)505.
21. H. Chen, Y. Guo, F. Wang, G. Wang and F. Yu, *New Carbon Mater.*, 32(2017)592.
22. Y. Li, W. Ou-Yang, X. Xu, M. Wang, S. Hou, T. Lu, Y. Yao and L. Pan, *Electrochim. Acta*, 271(2018)591.
23. Z. Tan, G. Chen and Y. Zhu, Carbon Based Supercapacitors Produced by the Activation of Graphene, *Nanocarbons for Advanced Energy Storage*, Wiley-Blackwell, 2011.
24. R. Wang, P. Wang, X. Yan, J. Lang, C. Peng and Q. Xue, *ACS Appl. Mater. Interfaces*, 4(2012)5800.
25. X. L. Su, S. H. Li, S. Jiang, Z. K. Peng, X. X. Guan and X. C. Zheng, *Adv. Powder Technol.*, (2018)S0921883118302322-.
26. X. Hao, J. Wang, B. Ding, Y. Wang, Z. Chang, H. Dou and X. Zhang, *J. Power Sources*, 352(2017)34.
27. C. Lu, Y. Huang, Y. Wu, J. Li, and J. Cheng, *J. Power Sources*, 394(2018)9.
28. H. Chen, Y. Guo, F. Wang, G. Wang and F. Yu, *New Carbon Mater.*, 32(2017)592.
29. M. F. El-Kady, V. Strong, S. Dubin and R. B. Kaner, *Science*, 335(2012)1326.
30. W. Li, F. Zhang, Y. Dou, Z. Wu, H. Liu, X. Qian, D. Gu, Y. Xia, B. Tu and D. Zhao, *Adv. Energy Mater.*, 1(2011)382.
31. H.Q. Wang, Y.L. Qing, Q.Y. Li, J.H. Yang and Q.F. Dai, *J. Phys. Chem. Solids*, 69 (2008) 2420.
32. L.Y. Pang, B. Zou, X. Han, L.Y. Cao, W. Wang, Y.P Guo, *Mater. Lett.*, 184 (2016) 88.